Magnetic excitations and continuum of a possibly field-induced quantum spin liquid in α−RuCl3

Zhe Wang, Stephan Reschke, D. Hüvonen, S.-H. Do, K.-Y. Choi, M. Gensch, U. Nagel, T. Rõõm, Alois Loidl

Angaben zur Veröffentlichung / Publication details:

Wang, Zhe, Stephan Reschke, D. Hüvonen, S.-H. Do, K.-Y. Choi, M. Gensch, U. Nagel, T. Rõõm, and Alois Loidl. 2017. "Magnetic excitations and continuum of a possibly field-induced quantum spin liquid in α−RuCl3." Physical Review Letters 119 (22): 227202. https://doi.org/10.1103/physrevlett.119.227202.

Magnetic Excitations and Continuum of a Possibly Field-Induced Quantum Spin Liquid in α-RuCl$_3$

Zhe Wang,[1] S. Reschke,[2] D. Hüvonen,[3] S.-H. Do,[4] K.-Y. Choi,[4] M. Gensch,[1] U. Nagel,[3] T. Rõõm,[3] and A. Loidl[2]
[1]*Institute of Radiation Physics, Helmholtz-Zentrum Dresden-Rossendorf, 01328 Dresden, Germany*
[2]*Experimental Physics V, Center for Electronic Correlations and Magnetism,*
Institute of Physics, University of Augsburg, 86135 Augsburg, Germany
[3]*National Institute of Chemical Physics and Biophysics, Akadeemia tee 23, 12618 Tallinn, Estonia*
[4]*Department of Physics, Chung-Ang University, Seoul 06974, Republic of Korea*

(Received 14 June 2017; revised manuscript received 8 August 2017; published 28 November 2017)

We report on terahertz spectroscopy of quantum spin dynamics in α-RuCl$_3$, a system proximate to the Kitaev honeycomb model, as a function of temperature and magnetic field. We follow the evolution of an extended magnetic continuum below the structural phase transition at $T_{s2} = 62$ K. With the onset of a long-range magnetic order at $T_N = 6.5$ K, spectral weight is transferred to a well-defined magnetic excitation at $\hbar\omega_1 = 2.48$ meV, which is accompanied by a higher-energy band at $\hbar\omega_2 = 6.48$ meV. Both excitations soften in a magnetic field, signaling a quantum phase transition close to $B_c = 7$ T, where a broad continuum dominates the dynamical response. Above B_c, the long-range order is suppressed, and on top of the continuum, emergent magnetic excitations evolve. These excitations follow clear selection rules and exhibit distinct field dependencies, characterizing the dynamical properties of a possibly field-induced quantum spin liquid.

DOI: 10.1103/PhysRevLett.119.227202

Quantum spin liquids (QSLs) are exotic states of matter in which quantum fluctuations prevent conventional magnetic long-range order even at the lowest temperatures. The ground states of QSLs are highly entangled and, albeit disordered, can exhibit well-defined quasiparticles, which are nonlocal and fractionalized [1,2]. The Kitaev honeycomb model [3] is a representative example for the existence of a QSL, which hosts fractionalized Majorana fermions and flux excitations. Moreover, bound states of the fractional excitations and excitations of the non-Abelian type can occur when the time-reversal symmetry is broken [4–6], e.g., by applying an external magnetic field. As this model is exactly solvable and thus provides a quantitative understanding for the ground state as well as for the dynamical response of the QSL [3,7], significant experimental efforts have been undertaken to realize the QSL and to search for its unconventional excitations.

Strong spin-orbit couplings together with a proper crystal electric field are important ingredients for realizing the Kitaev honeycomb model in magnetic insulators [8]. Based on $5d$ or $4d$ ions with strong spin-orbit coupling, a Mott insulator with an effective spin $1/2$ localized on a honeycomb lattice has been realized in the iridates [9] and recently in α-RuCl$_3$ [10–14]. In α-RuCl$_3$, besides the significant Kitaev term [15,16] that accounts for bond-dependent Ising exchange, other interactions, especially Heisenberg and off-diagonal exchange interactions, have been suggested to be responsible for the magnetic zigzag order below $T_N = 6.5$ K and for the observed sharp spin wave–like excitations [17–22].

To realize a QSL in α-RuCl$_3$, obviously the long-range zigzag order has to be suppressed, e.g., by tuning the external parameters, such as pressure [23,24] or the magnetic field [11,25–29]. When the external magnetic field is applied in the crystallographic ab plane of α-RuCl$_3$, the magnetic zigzag order is suppressed at about $B_c = 7$ T, with the emergence of a field-induced disordered phase, a putative QSL well below the fully polarized state. However, whether the elementary spin excitations are gapped or gapless, which is important for characterizing a QSL [1], is still under debate for the field-induced disordered phase in α-RuCl$_3$ [27,28], since a direct measurement of the magnetic excitations in the disordered phase so far has not been performed. Moreover, the existence of exotic quasiparticles is yet to be proven for the time-reversal symmetry-broken phase in applied magnetic fields.

Here, by performing terahertz spectroscopy as a function of temperature and magnetic field, we are able to directly reveal the quantum spin dynamics in the different phases of α-RuCl$_3$. We resolve a magnetic continuum at zero field, the evolvement of which is followed below the structural phase transition at $T_{s2} = 62$ K. Across the magnetic ordering temperature $T_N = 6.5$ K, the spectral weight of the continuum is partially shifted to two magnetic excitations. As a function of the magnetic field applied in the crystallographic ab plane, we provide spectroscopic evidence for a field-induced quantum phase transition at $B_c = 7$ T. Approaching B_c from below, the two magnetic excitations soften and we observe a remarkably broad continuum just at the critical field. Above B_c, magnetic excitations evolve out of the continuum, signaling the opening of a spin gap. The hierarchy and distinct field dependencies of the emergent excitations characterize the dynamical properties, which could be viewed as a signature of many-body interactions and/or bound states of fractionalized excitations [4–6] in the possibly field-induced QSL. Our experimental results also reveal a clear polarization dependence of these excitations, establishing a comprehensive characterization of the quantum spin dynamics of the QSL.

High-quality single crystals of α-RuCl$_3$ were grown using a vacuum sublimation method [16] and have been characterized by various techniques [14,25,30,31]. The samples for the optical experiments have a typical *ab* surface of 5×3 mm^2 and a thickness of about 1 mm. To study the temperature dependent optical response, time-domain terahertz transmission measurements were performed with the terahertz wave vector **k** perpendicular to the crystallographic *ab* plane, for 4–300 K in the effective spectral range 1.5–9 meV using a TPS Spectra 3000 spectrometer (TeraView Ltd.). Time domain signals were obtained for references (empty apertures) and samples, from which the power spectra were evaluated via a Fourier transformation [32,33]. Field dependent terahertz absorption experiments were carried out at 2.4 K in a Voigt configuration, i.e., $\mathbf{k} \perp \mathbf{B}$, with a magneto-optic cryostat equipped with a 17 T superconducting magnet. The absorption spectra were recorded using a Sciencetech SPS200 Martin-Puplett type spectrometer with a 0.3 K bolometer and a rotatable polarizer in front of the sample.

The terahertz response of α-RuCl$_3$ exhibits a very anomalous temperature dependence. Figure 1 shows the absorption coefficient as a function of temperature measured by heating and cooling the sample, for the photon energies $\hbar\omega_1 = 2.48$ meV and $\hbar\omega_2 = 6.38$ meV [see Fig. 2(a)]. For both frequencies we observe a markedly strong hysteresis between the heating and cooling curves for the temperature range from $T_{s2} = 62$ K to $T_{s1} = 166$ K, which reflects the structural phase transitions between the high-temperature monoclinic and the low-temperature rhombohedral phases [14,27,30,31].

Terahertz spectroscopy is sensitive to the dynamical response in the vicinity of the Γ point, where inelastic neutron scattering experiments have revealed a broad continuum of magnetic quasiparticles up to 120 K [16,19]. The evolution of this continuum with temperature was compared to an expected temperature dependence of the continuum of fractional Majorana fermions in the Kitaev model [16,34]. To avoid the complication of the structural fluctuations above T_{s2}, we show in Fig. 2(b) the absorption spectra below T_{s2} with the spectrum of 60 K taken as a reference. It has been indicated by other experimental techniques that below this temperature an evident magnetic-field dependent behavior develops [27,29]. Compared to the inelastic neutron scattering results, the terahertz spectroscopy reveals here a similar broad continuum extending over the spectral range up to 9 meV. With decreasing temperature the continuum develops rapidly and exhibits a broad maximum with the maximum position shifting to lower frequency. At 6 K (below T_N), the continuum is slightly reduced and the spectral weight is transferred to an excitation appearing at about 2.5 meV. The transfer of spectral weight to lower energies becomes more evident at lower temperatures. As seen from the 4.5 K spectrum, a very sharp peak shows up at 2.48 meV, while the continuum with a broad maximum at 5–6 meV is strongly suppressed. This behavior is also clearly displayed in Fig. 1. While the absorption coefficient at 2.48 meV increases below T_N, it drops slightly around 6.38 meV.

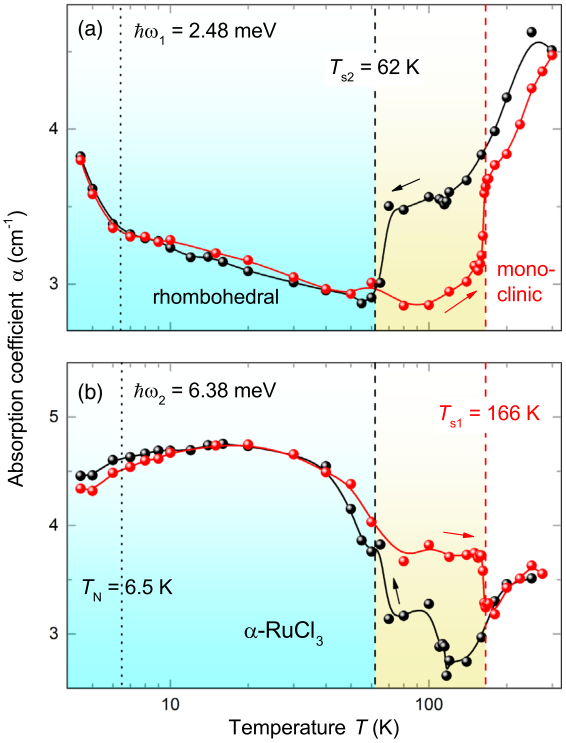

FIG. 1. Absorption coefficient α as a function of temperature T for the photon energies (a) $\hbar\omega_1 = 2.48$ meV and (b) $\hbar\omega_2 = 6.38$ meV, respectively, measured with the terahertz wave vector perpendicular to the crystallographic *ab* plane of α-RuCl$_3$. Clear hysteresis is revealed at the structural phase transitions between the low-temperature rhombohedral and the high-temperature monoclinic phases. The solid lines are guides for the eyes. The structural phase boundaries [14] are indicated by the dashed lines at $T_{s2} = 62$ K and $T_{s1} = 166$ K, and the magnetic phase transition by the dotted line at $T_N = 6.5$ K.

To unambiguously identify the magnetic excitations, we calculate the ratio of transmission as measured at 4.5 and 7 K, below and right above the magnetic ordering temperature T_N. As shown in Fig. 2(a), the ratio of transmission exhibits a sharp dip at 2.48 meV (mode M_1) and a shallow minimum around 6.38 meV (band M_2). Both modes, with frequencies comparable to that of the magnetic excitations determined in the inelastic neutron scattering experiments

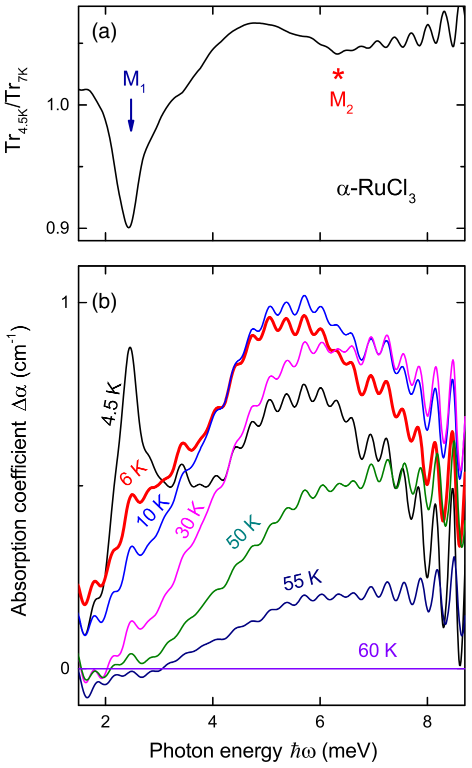

FIG. 2. (a) Ratio of transmission as obtained at 4.5 K ($T < T_N$) and 7 K ($T > T_N$) as a function of photon energy in α-RuCl$_3$. Two dips appear below $T_N = 6.5$ K at $\hbar\omega_1 = 2.48$ meV (mode M_1) and $\hbar\omega_2 = 6.38$ meV (band M_2), as marked by the arrow and asterisk, respectively. (b) Evolution of the absorption-coefficient spectra with decreasing temperature below T_{s2}, where the 60 K spectrum is taken as a reference. A broad continuum extending over the whole spectral range evolves with decreasing temperature down to T_N. Below T_N, the spectral weight transfers to lower frequency with a sharp peak developing at $\hbar\omega_1$. The oscillations are due to multiple interference at the sample surfaces.

[16,19], have been captured by the recent exact-diagonalization calculations [20] of a model guided by *ab initio* studies [21,35–37], where in addition to the Kitaev interactions, the off-diagonal couplings were included together with the nearest- and third-neighbor Heisenberg exchange interactions. However, the nature of the two modes remains unsettled. The lower-lying mode M_1 with a sharp absorption line, ascribed to the antiferromagnetic resonance in Ref. [38], corresponds to the single-magnon branch at the Γ point in the calculations [20]. In contrast, the band M_2 at higher energies is rather broad and weak. This mode may correspond to the higher-energy mode with a small intensity in the linear spin-wave theory [20]. Since M_1 and M_2 arise below the antiferromagnetic phase transition, they should naturally characterize the dynamical response of the zigzag order below T_N. Above T_N, the modes M_1 and M_2 transfer their spectral weight to the continuum as observed in the terahertz spectra [Fig. 2(b)]. The temperature dependence of the continuum is consistent with the results of the neutron scattering study [16,19], which has been discussed in the context of the Kitaev honeycomb model [19,34]. Alternatively, since the non-Kitaev terms are also important for α-RuCl$_3$ [18,20], one may speculate that this experimentally resolved continuum could correspond to a two-magnon continuum. Following this interpretation [20], the continuum represents incoherent excitations due to strong magnetic anharmonicity. In this case single magnons are unstable due to anharmonic interaction terms and the observation of a magnetic continuum in terahertz spectroscopy could be understood as a virtual process involving the excitation and decay of single magnons.

Figures 3(a) and 3(b) show the absorption spectra as a function of an external magnetic field applied in the *ab* plane, for the terahertz magnetic fields $\mathbf{h}^{\omega}\|\mathbf{B}$ and $\mathbf{h}^{\omega}\perp\mathbf{B}$, respectively. The spectra at 10 K in zero field are taken as the respective reference. For $\mathbf{h}^{\omega}\|\mathbf{B}$, the lower-lying mode $M_{1,\|}$ softens and becomes sharper in finite fields, together with the softening of the broad band $M_{2,\|}$ [see Fig. 3(c)]. At the critical field $B_c = 7$ T, the dynamical response is dominated by a broad continuum, extending over the whole resolvable spectra range, without any well-defined sharp excitations (the oscillations result from multiple interference at the sample surfaces). On further increasing the field, the broad continuum shifts to higher energies with two new excitations splitting off the continuum. At 9 T, the two excitations are observed at 2.7 and 4.4 meV, denoted by $L_{1,\|}$ and $L_{2,\|}$, respectively, and they can be well tracked and they shift to higher energies with an increasing magnetic field. The two modes $L_{1,\|}$ and $L_{2,\|}$ are well-defined excitations, whose line shapes become narrower on increasing fields.

The field dependence of these modes and the emergent continuum is represented in the contour plot of Fig. 3(c). The softening close to the critical field indicates that the spin gap is closed and another one is reopened, in agreement with the results obtained from other methods [26,27,29]. A very interesting feature of the field-induced disordered phase is the linear field dependence of the lower-lying mode $L_{1,\|}$. As shown in Fig. 3(c) this mode follows $\hbar\omega = \hbar\omega_0 + g^{*}\mu_B B\Delta S$ with an apparent g value of $g^{*} = 11.1(1)$ and the Bohr magneton μ_B, assuming a magnetic-dipole transition, i.e., $\Delta S = 1$. This suggests that a spin gap opens linearly with the magnetic field for the sector of the dynamical structure factor corresponding to $\mathbf{h}^{\omega}\|\mathbf{B}$. The linear opening of the spin gap is a feature expected for models beyond the Kitaev limit [39]. The apparent g^{*} factor revealed here is significantly larger than the value of $g_{ab} = 2.5$ estimated from the magnetization measurements [11] or $g_{ab} = 2.27$ estimated from the x-ray magnetic circular dichroism experiments [40], which is a reminiscence of the existence of bound states and many-body interactions in the possible QSL, as for the Heisenberg spin-1/2 chains [41,42].

For $\mathbf{h}^{\omega}\perp\mathbf{B}$ [Fig. 3(b)], approaching the critical field from below, the lower-lying mode $M_{1,\perp}$ first slightly hardens and

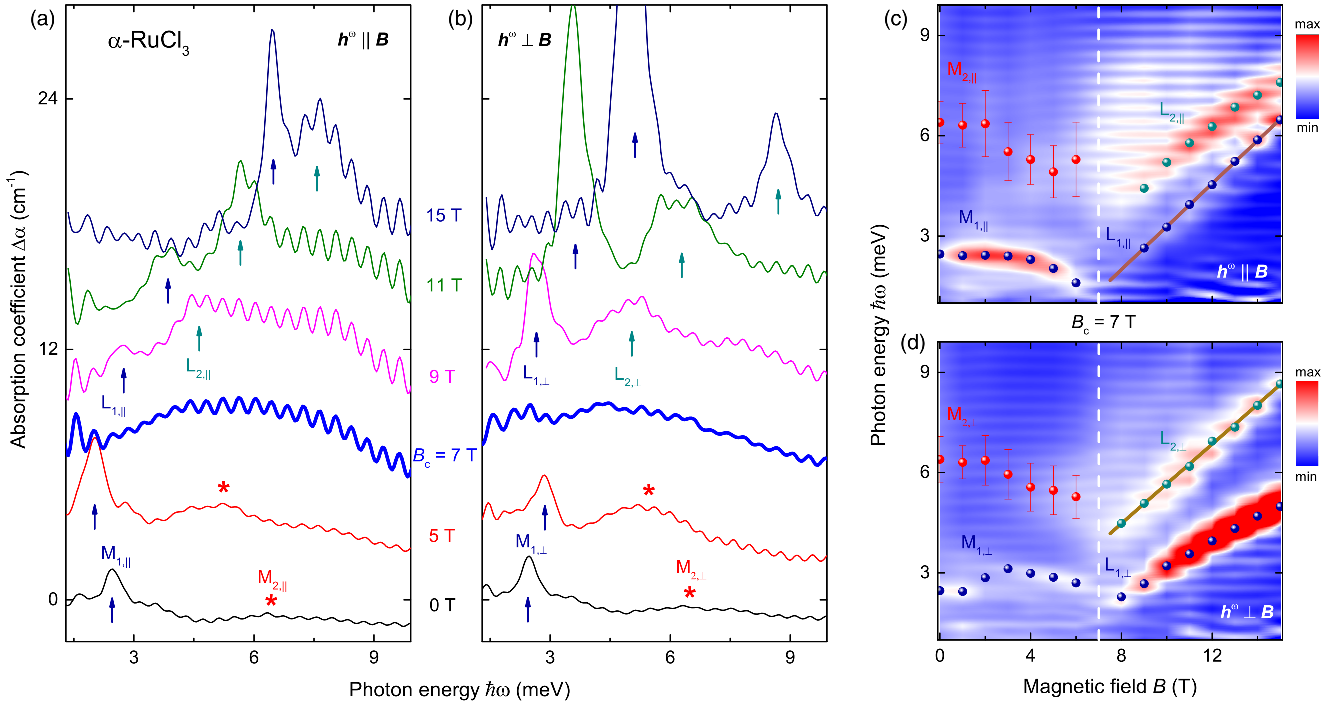

FIG. 3. Terahertz absorption spectra of α-RuCl$_3$ measured at 2.4 K below and above the critical field $B_c = 7$ T for (a) the terahertz magnetic field parallel ($\mathbf{h}^\omega \| \mathbf{B}$) and (b) perpendicular to the external magnetic field ($\mathbf{h}^\omega \perp \mathbf{B}$), respectively, with the spectra of 10 K taken as references. The spectra are shifted vertically by a constant for clarity. The arrows indicate the low-energy magnetic excitations with sharp absorption lines, while the asterisks mark the high-energy excitations that are rather broad. At the critical field, a broad continuum is observed that extends over the whole spectral range. Above B_c, various excitations emerge on the top of the continuum. (c), (d) Contour plot of the absorption coefficient as a function of field and photon energy for $\mathbf{h}^\omega \| \mathbf{B}$ and $\mathbf{h}^\omega \perp \mathbf{B}$. The symbols correspond to the peak positions of the low-energy modes and the maximum positions of the high-energy bands in (a) and (b). For the broad bands, the linewidths are indicated by the error bars. Above B_c, for $\mathbf{h}^\omega \| \mathbf{B}$ the lower-lying mode $L_{1,\|}$ follows a linear field dependence with an apparent g value of $g^* = 11.1(1)$ assuming a magnetic-dipole excitation [solid line in (c)], while for $\mathbf{h}^\omega \perp \mathbf{B}$ the field dependence of the higher-lying mode $L_{2,\perp}$ is described by the linear Zeeman term with $g^* = 10.2(2)$ [solid line in (d)]. The vertical dashed line marks the critical field $B_c = 7$ T.

then softens, while the band $M_{2,\perp}$ softens monotonically. At the critical field, the spectrum is again dominated by a broad continuum extending over the whole spectral range. Above B_c one can identify two sharp modes $L_{1,\perp}$ and $L_{2,\perp}$, both emerging on top of the continuum and shifting to higher energies together with the continuum. The absorption lines of the two modes become sharper with increasing field. In addition, the continuum is suppressed in high fields and the spectral weight is transferred to the low-lying modes. In the contour plot of Fig. 3(d) one can readily see these field-dependent features.

The emergent magnetic excitations and continuum of the field-induced quantum disordered phase exhibit a clear contrast between $\mathbf{h}^\omega \perp \mathbf{B}$ and $\mathbf{h}^\omega \| \mathbf{B}$. Both the eigenenergies and their field dependences are different for the two polarizations, revealing the contrast of the two different sectors of dynamical structure factors. For $\mathbf{h}^\omega \perp \mathbf{B}$ the lower-lying mode $L_{1,\perp}$ has lower eigenenergies, and the absorption lines are much sharper and stronger than those of its counterpart $L_{1,\|}$. Moreover, the eigenenergy of $L_{1,\perp}$ does not follow a linear field dependence, but shows a slower increase with increasing field. The slower increase is consistent with the results of low-temperature specific heat measurements (below 3 K) [25] where the thermodynamics is presumably dominated by the lowest-lying excitations. In contrast, the mode $L_{2,\perp}$ in the sector of $\mathbf{h}^\omega \perp \mathbf{B}$ can be described by the linear Zeeman term with $g^* = 10.2(2)$, while the $L_{2,\|}$ mode hardens evidently slower than linearly with the field, although these two modes have similar linewidths. These modes could be the bound states of fractionalized excitations [4–6], which are narrow and can evolve from the excitation continuum as the time-reversal symmetry is broken by the applied magnetic field [43]. It is worth noting that the continuum emerging at the quantum phase transition has been confirmed by a recent inelastic neutron scattering study [44], and the linear field dependency in the quantum disordered phase has recently also been revealed by electron spin resonance spectroscopy [45] and captured by very recent exact-diagonalization calculations [46] that predict the magnetic excitations evolving in magnetic fields above the quantum phase transition.

To conclude, terahertz spectroscopy as a function of temperature and magnetic field reveals emergent magnetic excitations and continua in a possibly field-induced QSL in α-RuCl$_3$. While two magnonic excitations evolving on top of a continuum are resolved in the magnetically ordered phase and well below the critical field, the QSL is dynamically characterized by an emergent continuum at the quantum criticality and various magnetic excitations with distinct field and polarization dependencies above the quantum phase transition. Our results pave the way to understand the dynamical behavior of the QSL and provide constraints for a quantitative theoretical description, e.g., via the identification of a realistic model or by extending the Kitaev model with terms breaking the time-reversal symmetry.

We would like to thank Seung-Ho Baek, Lukas Janssen, Johannes Knolle, Roderich Moessner, Roser Valentí, Jinsheng Wen, Stephen M. Winter, Liang Wu, Yi-Zhuang You, and Xenophon Zotos for helpful discussions. This work has been partially supported by the Deutsche Forschungsgemeinschaft via the Transregional Research Collaboration TRR 80: From Electronic Correlations to Functionality (Augsburg-Munich-Stuttgart), and a Korea Research Foundation (KRF) grant, funded by the Korean Government (MEST) (Grant No. 20160874). The work in Tallinn was supported by the Estonian Ministry of Education and Research under Grant No. IUT23-03, the Estonian Research Council Grant No. PUT451, and the European Regional Development Fund Project No. TK134.

[1] L. Savary and L. Balents, Quantum spin liquids: a review, Rep. Prog. Phys. **80**, 016502 (2017).

[2] L. Balents, Spin liquids in frustrated magnets, Nature (London) **464**, 199 (2010).

[3] A. Kitaev, Anyons in an exactly solved model and beyond, Ann. Phys. (Amsterdam) **321**, 2 (2006).

[4] J. Knolle, D. L. Kovrizhin, J. T. Chalker, and R. Moessner, Dynamics of fractionalization in quantum spin liquids, Phys. Rev. B **92**, 115127 (2015).

[5] V. Lahtinen, A. W. W. Ludwig, and S. Trebst, Perturbed vortex lattices and the stability of nucleated topological phases, Phys. Rev. B **89**, 085121 (2014).

[6] H. Théveniaut and M. Vojta, Bound states of fractionalized excitations in a modulated Kitaev spin liquid, Phys. Rev. B **96**, 054401 (2017).

[7] J. Knolle, D. L. Kovrizhin, J. T. Chalker, and R. Moessner, Dynamics of a Two-Dimensional Quantum Spin Liquid: Signatures of Emergent Majorana Fermions and Fluxes, Phys. Rev. Lett. **112**, 207203 (2014).

[8] G. Jackeli and G. Khaliullin, Mott Insulators in the Strong Spin-Orbit Coupling Limit: From Heisenberg to a Quantum Compass and Kitaev Models, Phys. Rev. Lett. **102**, 017205 (2009).

[9] Y. Singh, S. Manni, J. Reuther, T. Berlijn, R. Thomale, W. Ku, S. Trebst, and P. Gegenwart, Relevance of the Heisenberg-Kitaev Model for the Honeycomb Lattice Iridates A_2IrO$_3$, Phys. Rev. Lett. **108**, 127203 (2012).

[10] K. W. Plumb, J. P. Clancy, L. J. Sandilands, V. V. Shankar, Y. F. Hu, K. S. Burch, Hae-Young Kee, and Young-June Kim, α-RuCl$_3$: A spin-orbit assisted Mott insulator on a honeycomb lattice, Phys. Rev. B **90**, 041112(R) (2014).

[11] Y. Kubota, H. Tanaka, T. Ono, Y. Narumi, and K. Kindo, Successive magnetic phase transitions in α-RuCl$_3$: XY-like frustrated magnet on the honeycomb lattice, Phys. Rev. B **91**, 094422 (2015).

[12] R. D. Johnson, S. C. Williams, A. A. Haghighirad, J. Singleton, V. Zapf, P. Manuel, I. I. Mazin, Y. Li, H. O. Jeschke, R. Valentí, and R. Coldea, Monoclinic crystal structure of α-RuCl$_3$ and the zigzag antiferromagnetic ground state, Phys. Rev. B **92**, 235119 (2015).

[13] H. B. Cao, A. Banerjee, J.-Q. Yan, C. A. Bridges, M. D. Lumsden, D. G. Mandrus, D. A. Tennant, B. C. Chakoumakos, and S. E. Nagler, Low-temperature crystal and magnetic structure of α-RuCl$_3$, Phys. Rev. B **93**, 134423 (2016).

[14] S.-Y. Park, S.-H. Do, K.-Y. Choi, D. Jang, T.-H. Jang, J. Schefer, C.-M. Wu, J. S. Gardner, J. M. S. Park, J.-H. Park, and Sungdae Ji, Emergence of the isotropic Kitaev honeycomb lattice with two-dimensional Ising universality in α-RuCl$_3$, arXiv:1609.05690.

[15] L. J. Sandilands, Y. Tian, K. W. Plumb, Y.-J. Kim, and K. S. Burch, Scattering Continuum and Possible Fractionalized Excitations in α-RuCl$_3$, Phys. Rev. Lett. **114**, 147201 (2015).

[16] S.-H. Do, S.-Y. Park, J. Yoshitake, J. Nasu, Y. Motome, Y. S. Kwon, D. T. Adroja, D. J. Voneshen, K. Kim, T.-H. Jang, J.-H. Park, K.-Y. Choi, and S. Ji, Majorana fermions in the Kitaev quantum spin system α-RuCl$_3$, Nat. Phys. **13**, 1079 (2017).

[17] A. Banerjee, C. A. Bridges, J.-Q. Yan, A. A. Aczel, L. Li, M. B. Stone, G. E. Granroth, M. D. Lumsden, Y. Yiu, J. Knolle, S. Bhattacharjee, D. L. Kovrizhin, R. Moessner, D. A. Tennant, D. G. Mandrus, and S. E. Nagler, Proximate Kitaev quantum spin liquid behaviour in a honeycomb magnet, Nat. Mater. **15**, 733 (2016).

[18] K. Ran, J. Wang, W. Wang, Z.-Y. Dong, X. Ren, S. Bao, S. Li, Z. Ma, Y. Gan, Y. Zhang, J. T. Park, G. Deng, S. Danilkin, S.-L. Yu, J.-X. Li, and J. Wen, Spin-Wave Excitations Evidencing the Kitaev Interaction in Single Crystalline α-RuCl$_3$, Phys. Rev. Lett. **118**, 107203 (2017).

[19] A. Banerjee, J. Yan, J. Knolle, C. A. Bridges, M. B. Stone, M. D. Lumsden, D. G. Mandrus, D. A. Tennant, R. Moessner, and S. E. Nagler, Neutron tomography of magnetic Majorana fermions in a proximate quantum spin liquid, Science **356**, 1055 (2017).

[20] S. M. Winter, K. Riedl, A. Honecker, and R. Valentí, Breakdown of magnons in a strongly spin-orbital coupled magnet, Nat. Commun. **8**, 1152 (2017).

[21] S. M. Winter, Y. Li, H. O. Jeschke, and R. Valentí, Challenges in design of Kitaev materials: Magnetic interactions from competing energy scales, Phys. Rev. B **93**, 214431 (2016).

[22] L. Janssen, E. C. Andrade, and M. Vojta, Honeycomb-Lattice Heisenberg-Kitaev Model in a Magnetic Field: Spin Canting, Metamagnetism, and Vortex Crystals, Phys. Rev. Lett., **117**, 277202 (2016).

[23] Z. Wang, J. Guo, F. F. Tafti, A. Hegg, S. Sen, V. A. Sidorov, L. Wang, S. Cai, W. Yi, Y. Zhou, H. Wang, S. Zhang, K. Yang, A. Li, X. Li, Y. Li, J. Liu, Y. Shi, W. Ku, Q. Wu, R. J. Cava, and L. Sun, Observation of the quantum spin liquid state in pressurized α-RuCl$_3$, arXiv:1705.06139.

[24] Y. Cui, J. Zheng, K. Ran, J. Wen, Z. Liu, B. Liu, W. Guo, and W. Yu, A pressure-induced quantum disordered phase in α-RuCl$_3$ evidenced by NMR, arXiv:1706.02697.

[25] A. U. B. Wolter, L. T. Corredor, L. Janssen, K. Nenkov, S. Schönecker, S.-H. Do, K.-Y. Choi, R. Albrecht, J. Hunger, T. Doert, M. Vojta, and B. Büchner, Field-induced quantum criticality in the Kitaev system α-RuCl$_3$, Phys. Rev. B **96**, 041405(R) (2017).

[26] J. A. Sears, Y. Zhao, Z. Xu, J. W. Lynn, and Y. J. Kim, Phase diagram of α-RuCl$_3$ in an in-plane magnetic field, Phys. Rev. B **95**, 180411 (2017).

[27] S.-H. Baek, S.-H. Do, K.-Y. Choi, Y. S. Kwon, A. U. B. Wolter, S. Nishimoto, J. van den Brink, and B. Büchner, Evidence for a Field-Induced Quantum Spin Liquid in α-RuCl$_3$, Phys. Rev. Lett. **119**, 037201 (2017).

[28] J. Zheng, K. Ran, T. Li, J. Wang, P. Wang, B. Liu, Z. Liu, B. Normand, J. Wen, and W. Yu, Gapless spin excitations in the field-induced quantum spin liquid phase of α-RuCl$_3$, arXiv:1703.08474.

[29] R. Hentrich, A. U. B. Wolter, X. Zotos, W. Brenig, D. Nowak, A. Isaeva, T. Doert, A. Banerjee, P. Lampen-Kelley, D. G. Mandrus, S. E. Nagler, J. Sears, Y.-J. Kim, B. Büchner, and Ch. Hess, Large field-induced gap of Kitaev-Heisenberg paramagnons in α-RuCl$_3$, arXiv:1703.08623.

[30] A. Glamazda, P. Lemmens, S.-H. Do, Y. S. Kwon, and K.-Y. Choi, Relation between Kitaev magnetism and structure in α-RuCl$_3$, Phys. Rev. B **95**, 174429 (2017).

[31] S. Reschke, F. Mayr, Z. Wang, S.-H. Do, K.-Y. Choi, and A. Loidl, Electronic and phonon excitations in α-RuCl$_3$, Phys. Rev. B **96**, 165120 (2017).

[32] Zhe Wang, M. Schmidt, A. K. Bera, A. T. M. N. Islam, B. Lake, A. Loidl, and J. Deisenhofer, Spinon confinement in the one-dimensional Ising-like antiferromagnet SrCo$_2$V$_2$O$_8$, Phys. Rev. B **91**, 140404(R) (2015).

[33] See Supplemental Material at http://link.aps.org/supplemental/10.1103/PhysRevLett.119.227202 for the time-domain signals.

[34] J. Yoshitake, J. Nasu, and Y. Motome, Fractional Spin Fluctuations as a Precursor of Quantum Spin Liquids: Majorana Dynamical Mean-Field Study for the Kitaev Model, Phys. Rev. Lett. **117**, 157203 (2016).

[35] R. Yadav, N. A. Bogdanov, V. M. Katukuri, S. Nishimoto, J. van den Brink, and L. Hozoi, Kitaev exchange and field-induced quantum spin-liquid states in honeycomb α-RuCl$_3$, Sci. Rep. **6**, 37925 (2016).

[36] W. Wang, Z.-Y. Dong, S.-L. Yu, and J.-X. Li, Theoretical investigation of the magnetic dynamics and superconducting pairing symmetry in α-RuCl$_3$, Phys. Rev. B **96**, 115103 (2017).

[37] Y. S. Hou, H. J. Xiang, and X. G. Gong, Unveiling magnetic interactions of ruthenium trichloride via constraining direction of orbital moments: Potential routes to realize quantum spin liquid, Phys. Rev. B **96**, 054410 (2017).

[38] A. Little, L. Wu, P. Lampen-Kelley, A. Banerjee, S. Pantankar, D. Rees, C. A. Bridges, J.-Q. Yan, D. Mandrus, S. E. Nagler, and J. Orenstein, Antiferromagnetic resonance and terahertz conductivity in α-RuCl$_3$, arXiv:1704.07357.

[39] X.-Y. Song, Y.-Z. You, and L. Balents, Low-Energy Spin Dynamics of the Honeycomb Spin Liquid Beyond the Kitaev Limit, Phys. Rev. Lett. **117**, 037209 (2016).

[40] S. Agrestini, C.-Y. Kuo, K.-T. Ko, Z. Hu, D. Kasinathan, H. B. Vasili, J. Herrero-Martin, S. M. Valvidares, E. Pellegrin, L.-Y. Jang, A. Henschel, M. Schmidt, A. Tanaka, and L. H. Tjeng, Electronically highly cubic conditions for Ru in α-RuCl$_3$, Phys. Rev. B **96**, 161107(R) (2017).

[41] Z. Wang, J. Wu, W. Yang, A. K. Bera, D. Kamenskyi, A. T. M. N. Islam, S. Xu, J. M. Law, B. Lake, C. Wu, and A. Loidl, Experimental observation of Bethe strings, arXiv:1706.04181.

[42] W. Yang, J. Wu, S. Xu, Z. Wang, and C. Wu, Quantum spin dynamics of the axial antiferromagnetic spin-$1/2$ XXZ chain in a longitudinal magnetic field, arXiv:1702.01854.

[43] J. Knolle, *Dynamics of a Quantum Spin Liquid* (Springer, New York, 2016), Chap. 5.

[44] A. Banerjee, P. Lampen-Kelley, J. Knolle, C. Balz, A. A. Aczel, B. Winn, Y. Liu, D. Pajerowski, J.-Q. Yan, C. A. Bridges, A. T. Savici, B. C. Chakoumakos, M. D. Lumsden, D. A. Tennant, R. Moessner, D. G. Mandrus, and S. E. Nagler, Excitations in the field-induced quantum spin liquid state of α-RuCl$_3$, arXiv:1706.07003.

[45] A. N. Ponomaryov, E. Schulze, J. Wosnitza, P. Lampen-Kelley, A. Banerjee, J.-Q. Yan, C. A. Bridges, D. G. Mandrus, S. E. Nagler, A. K. Kolezhuk, and S. A. Zvyagin, Direct observation of the field-induced gap in the honeycomb-lattice material α-RuCl$_3$, arXiv:1706.07240.

[46] S. M. Winter, K. Riedl, D. Kaib, R. Coldea, and R. Valentí, Probing α-RuCl$_3$ beyond magnetic order: Effects of temperature and magnetic field, arXiv:1707.08144.